# Solvent-mediated conformational similarities within a series of 1D coordination polymers constructed from a new flexible ditopic bis-imidazole ligand†‡

**Storm V. Potts and Leonard J. Barbour***

*Received (in Victoria, Australia) 11th May 2010, Accepted 23rd June 2010*
**DOI: 10.1039/c0nj00357c**

A novel conformationally flexible ditopic ligand 1,3-bis(1-imidazolyl-2-thione)-2,4,6-trimethylbenzene (**L**), bearing thioether linkages between a central aromatic moiety and two pendant imidazole rings, was synthesised. Treatment of **L** with $CdI_2$ under varying conditions afforded four new solvates, $\{[Cd\mathbf{L}I_2]\cdot H_2O\}_n$, $\{[Cd\mathbf{L}I_2]\cdot CH_3OH\}_n$, $\{[Cd\mathbf{L}I_2]\cdot 2CH_3CN\}_n$, and $\{[Cd\mathbf{L}I_2]\cdot 2CH_3OH\}_n$, which were characterised by single crystal X-ray diffraction. In all four of the complexes the Cd metal centers are tetrahedrally coordinated to two iodide ions and two nitrogen atoms from separate **L** molecules to form continuous 1D polymeric strands. The solvent molecules participate in strong hydrogen bonding with the amino nitrogen atoms of the imidazole rings. Hirshfeld surface analysis and breakdown of the corresponding 2D fingerprint plots of the four structures provide a convenient means of quantifying the interactions within the crystal structures, revealing significant similarities in the interactions experienced by each complex.



## Introduction

Transition-metal based supermolecules have been recognised for their potential use in optics,[1] gas sorption[2] and catalysis,[3] but control of the architectures derived from the self-assembly of transition metal salts and flexible organic bridging ligands remains an elusive aspect of crystal engineering.[4] To date, most metal–organic frameworks have been constructed using rigid ligands (mostly containing pyridyl and carboxylate functionalities) owing to the relative ease of prediction of the resulting networks and the limited conformational changes that can occur. However, the interest in comparatively flexible organic bridging ligands is on the rise because the conformational diversity of these ligands could facilitate the discovery of unique frameworks, and thus contribute further understanding of the manner in which supramolecular architectures assemble.[5]

Imidazole functionalised compounds constitute a class of N-donor organic ligands that have attracted increasing attention owing to their high affinity for metals and their relative ease of preparation.[6] Indeed, we[7] and others[8] have shown that imidazole-based bridging ligands have a rich coordination chemistry that can be successfully exploited to construct a range of coordination networks with interesting topologies and properties.

As part of our ongoing interest in the supramolecular structures derived from the reaction of imidazole-functionalised ligands and transition metals, we have prepared a novel ditopic ligand bearing thioether linkages between a central aromatic moiety and two pendant imidazole rings, namely 1,3-bis(1-imidazolyl-2-thione)-2,4,6-trimethylbenzene (**L**, Scheme 1). Herein, we report the synthesis and crystal structures of four new solvates of one dimensional (1D) Cd(II) coordination polymers constructed from **L** and $CdI_2$.

We note that variation of the solvent, as well as the solvent-to-complex ratio results in subtle changes in the packing of the 1D chains. In addition to conventional packing analysis, we have also inspected the intermolecular interactions in the crystal structures by means of Hirshfeld surface analysis[9] and by considering the characteristic regions of the corresponding 2D fingerprint plots for an individual complex in each structure.[10]

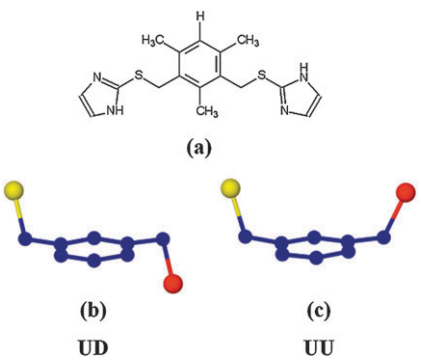


**Scheme 1** (a) 1,3-Bis(1-imidazolyl-2-thione)-2,4,6-trimethylbenzene (**L**). (b) In the **UD** conformation the two imidazolyl rings (represented as yellow and red spheres respectively) are situated on the opposite sides and (c) in the **UU** conformation they are situated on the same side of the aromatic core plane.

*Department of Chemistry, University of Stellenbosch, Stellenbosch 7600, South Africa. E-mail: ljb@sun.ac.za; Fax: +27 21 808 3360; Tel: +27 21 808 3335*

† This article is part of a themed issue on Coordination polymers: structure and function.

‡ CCDC reference numbers 776909–776912. For crystallographic data in CIF or other electronic format see DOI: 10.1039/c0nj00357c

## Results and discussion

The bidentate ligand **L** was synthesized by the $SN_2$ reaction of 2-mercaptoimidazole with 2,4-bis(chloromethyl)-1,3,5-trimethylbenzene in MeOH. Although the imidazolyl rings and aromatic core are rigid, the connections between the two "arms" and the core (*i.e.* the methylene group and sulfur bridge) allow the arms to rotate freely in solution. Owing to this flexibility the ligand can assume a **UU** (or up–up) conformation, where the two imidazolyl rings are situated on the same side of the central aromatic core, or a **UD** (up–down) conformation, where the two rings are positioned on opposite sides of the core (Scheme 1b and c). Diffraction-quality single crystals of complexes **1**, **2** and **4** (Fig. 1) were obtained by the reaction of **L** with $CdI_2$ (in ligand-to-metal molar ratios of 1 : 1, 2 : 1 and 1 : 2, respectively) in MeOH, followed by slow evaporation of the solvent. Single crystals of complex **3** were obtained from a 1 : 1 solution of **L** and $CdI_2$ in MeCN, followed by slow evaporation of the solvent.

### Structural analysis of complexes 1–4

**$\{[CdLI_2]\cdot H_2O\}_n$ (1).** Single crystal X-ray diffraction analysis reveals that complex **1** forms a 1D strand propagating along [010]. Adjacent Cd-ions are connected by means of a single ligand **L** in the **UU** conformation and the dihedral angles between the planes of the two imidazole rings and the benzene ring are 28.5(1)° and 30.3(2)°. Each metal center is coordinated to two iodine ions and two nitrogen atoms from separate ligand molecules to form a distorted tetrahedral coordination environment around each metal ion. The coordinating angles range from 101.38(9)° to 116.74(2)° and the parameters relevant to the coordination geometries are given in Table 1.

In addition to the constituents that form part of the 1D chain, the asymmetric unit (ASU) also contains one water molecule. The two imidazole amino nitrogen atoms belonging to the same ligand molecule simultaneously donate two hydrogen bonds to this water molecule, thus stabilizing the overall **UU** conformation of the ligand (Table 2). Neighbouring

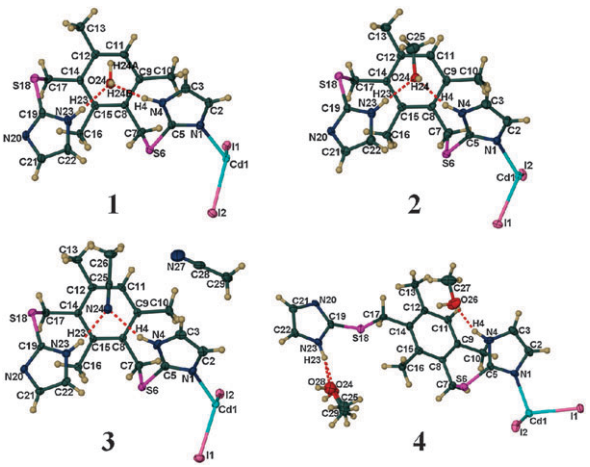


**Fig. 1** Atomic displacement (50% probability plots) showing the asymmetric units of complexes **1–4**. Hydrogen atoms are shown as spheres of arbitrary radius and hydrogen bonds are shown as dashed red lines. In the case of **4**, one of the methanol molecules is disordered over two sites as shown.

**Table 1** Coordination geometric parameters for complexes **1–4**

| | **1** | **2** | **3** | **4** |
|---|---|---|---|---|
| Bond lengths (Å) | | | | |
| Cd1–I1 | 2.7575(6) | 2.7720(5) | 2.7332(5) | 2.7482(7) |
| Cd1–I2 | 2.7564(6) | 2.6844(5) | 2.7341(5) | 2.7424(7) |
| Cd1–N1 | 2.221(3) | 2.253(4) | 2.240(4) | 2.223(5) |
| Cd1–N20$^i$ | 2.239(3) | 2.265(4) | 2.268(4) | 2.226(5) |
| Bond angles (°) | | | | |
| I2–Cd1–I1 | 116.74(2) | 119.718(17) | 115.638(18) | 120.28(2) |
| N1–Cd1–I1 | 106.62(9) | 102.63(9) | 112.88(11) | 101.48(13) |
| N20$^i$–Cd1–I1 | 107.08(9) | 101.34(9) | 104.62(11) | 106.82(13) |
| N1–Cd1–I2 | 114.50(9) | 120.63(9) | 114.25(11) | 107.47(12) |
| N20$^i$–Cd1–I2 | 101.38(9) | 110.51(9) | 107.13(10) | 103.73(13) |
| N1–Cd1–N20$^i$ | 110.14(13) | 98.44(13) | 100.43(15) | 117.94(19) |

Symmetry codes for **1**: (*i*) $x, y-1, z$; for **2**: (*i*) $x, y+1, z$; for **3**: (*i*) $x, y+1, z$; for **4**: (*i*) $x, -y+2, z+\frac{1}{2}$.

**Table 2** Hydrogen-bond geometry for complexes **1–4**

| D–H···*A* | D···*A* | D–H···*A* | D···*A* |
|---|---|---|---|
| **1** | | **3** | |
| N4–H4···O24 | 2.811(5) | N4–H4···N24 | 2.901(6) |
| N23–H23···O24 | 2.768(5) | N23–H23···N24 | 2.909(6) |
| O24–H24A···I1$^i$ | 3.508(3) | | |
| O24–H24B···I2$^i$ | 3.589(3) | | |
| **2** | | **4** | |
| N4–H4···O24 | 2.836(5) | N4–H4···O26 | 2.713(8) |
| N23–H23···O24 | 2.812(5) | N23–H23···O24 | 2.723(10) |
| O24–H26···I1$^{ii}$ | 3.436(3) | O26–H26···I2$^{iii}$ | 3.441(5) |
| | | O28–H28···I1$^{iv}$ | 3.421(12) |

Symmetry codes: (*i*) $x, -y+\frac{3}{2}, z-\frac{1}{2}$; (*ii*) $-x+\frac{3}{2}, -y+\frac{1}{2}, -z+1$; (*iii*) $x, y+1, z$; (*iv*) $1-x, 1+y, \frac{3}{2}-z$. Parameters involving hydrogen atoms have not been included since their positions are not reliable.

1D strands are connected to form a distorted 2D honeycomb arrangement by the donation of two hydrogen bonds from the water molecule to the coordinated iodine atoms (Fig. 2, top). The honeycomb layer is connected to another layer by means of offset face-to-face π–π interactions between neighbouring benzene rings (centroid–centroid distance = 3.569 Å) and, as a result, the honeycomb layers stack on top of one another such that the atoms of the first layer eclipse those of the third layer when viewed along [100] (Fig. 2, bottom).

**$\{[CdLI_2]\cdot CH_3OH\}_n$ (2).** The ASU of **2** is similar to that of **1** both in terms of its constituents as well as the relative arrangement of its components (Fig. 1). However, in **2** a methanol molecule occupies the position of the water molecule in **1**, assuming the role of a bifurcated hydrogen bond acceptor to the nitrogen donors of the imidazole groups to stabilize the **UU** conformation of the ligand. The dihedral angles between the planes of the two imidazole rings and that of the phenylene ring are 31.8(3)° and 37.6(2)°, respectively. The unique angles that complete the distorted tetrahedral environment around the Cd metal center range from 98.44(1)° to 120.63(9)° and successive metal centers are linked to one another *via* individual ligand molecules to form a 1D polymeric chain running parallel to [010]. The methanol molecule donates a hydrogen bond to one of the ligated iodide ions of an adjacent strand (Fig. 3), thus connecting adjacent 1D chains into bilayers (see Table 2 for hydrogen bonding parameters).

 

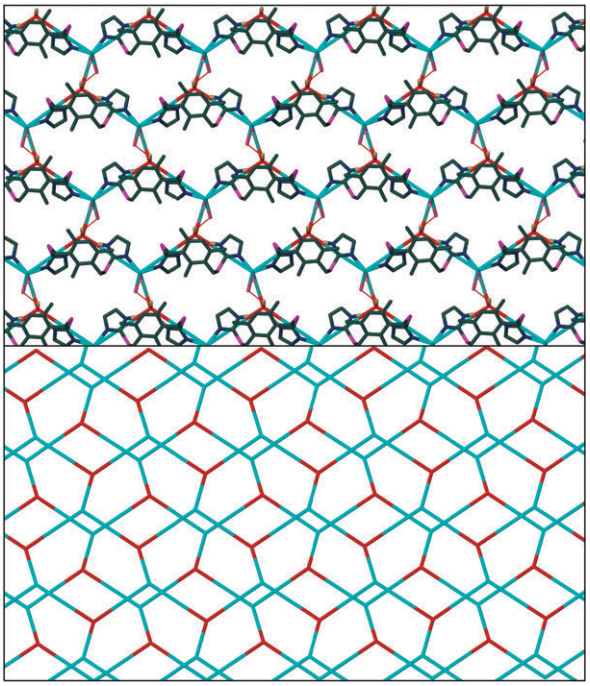

**Fig. 2** Distorted 2D honeycomb layer (top) formed by hydrogen bonding in **1**. Molecules are shown in the ball-and-stick metaphor. A simplification of the 2D honeycomb layers (bottom) shows the *...ABAB...* stacking arrangement. Both projections are viewed along [100].

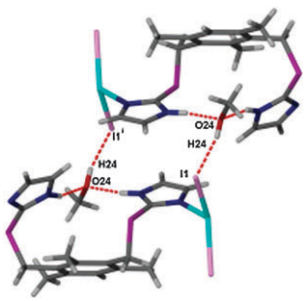


**Fig. 3** Capped-stick representation showing the hydrogen bonds formed in **2**. Atoms of the fragment at the top are related to those at the bottom by the symmetry operation $3/2 - x$, $1/2 - y$, $1 - z$. Hydrogen bonds are shown as dashed red lines.

Fig. 4 shows the 2D assembly in which the bilayers are connected to one another by π–π stacking interactions between adjacent benzene rings (centroid–centroid distance = 4.112 Å).

**{[CdLI$_2$]·2CH$_3$CN}$_n$ (3).** Complex **3** also features **L** in the **UU** conformation. The ASU is similar to that of the previous two structures, except that it contains two acetonitrile solvent molecules (Fig. 1). As observed in **1** and **2**, one solvent molecule acts as a bifurcated hydrogen bond acceptor for the amino nitrogen donors of the imidazole groups (Table 2). Complex **3** forms 1D strands similar to those of **1** and **2**; these strands also run parallel to [010] (Fig. 5).

All neighbouring strands interact with one another by means of weak offset face-to-face π–π interactions between

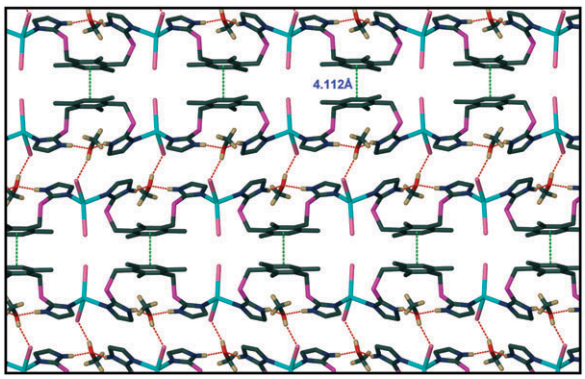


**Fig. 4** Packing arrangement of the 2D layers formed in **2**, as viewed along [010]. Molecules are shown in the capped-stick metaphor; hydrogen bonds and π–π stacking interactions are shown as dashed red and green lines, respectively.

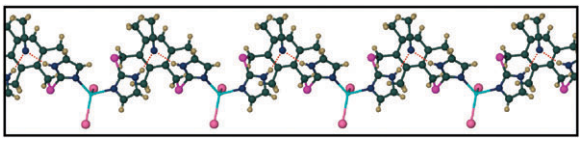

**Fig. 5** Ball-and-stick plot showing the 1D strand formed in **3**, as viewed down [100]. Hydrogen bonds are shown as dashed red lines.

phenylene (centroid–centroid distance = 3.818 Å) and imidazole (centroid–centroid distances of 3.538 Å and 3.794 Å apply) rings to form 2D sheets running parallel to (100) (Fig. 6).

**{[CdLI$_2$]·2CH$_3$OH}$_n$ (4).** The ASU of **4** consists of one ligand **L**, two iodine ions and two methanol molecules (see Fig. 1). One of the methanol molecules is disordered over two positions. The Cd ion is coordinated to two iodine counter-ions and two imidazole nitrogen atoms of separate **L** molecules. This results in a distorted tetrahedral coordination geometry around the metal ion (coordinating angles range from 101.48(13)° to 120.28(2)°). Neighbouring metal centres are connected to each other *via* a single ligand **L** to form a 1D zigzag polymeric strand running parallel to [101] (Fig. 7). Each ligand assumes the **UD** conformation with the coordinating

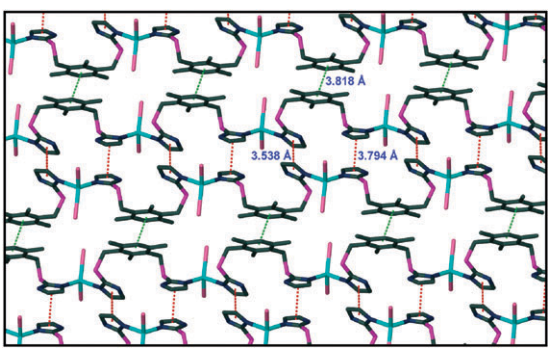


**Fig. 6** Capped-stick representation of the 2D layers formed in **3** as viewed along [100]. Hydrogen atoms and solvent molecules have been omitted for clarity and π–π stacking interactions have been shown as dashed green and red lines between phenylene and imidazole rings, respectively.

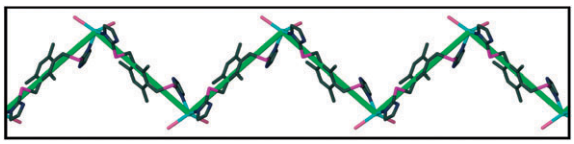

**Fig. 7** A single 1D strand of **4** running parallel to [101]; thick green lines are shown to emphasise the zigzag character of the strand; molecules are shown in the capped-stick metaphor.

nitrogen atoms of the imidazole groups oriented in opposite directions. The dihedral angles between the imidazole and benzene ring planes are 37.9(3)° (for the ring containing N1) and 5.2(5)° (for the ring containing N20).

Each methanol molecule accepts a hydrogen bond from an uncoordinated imidazole nitrogen atom. One of these methanol molecules then donates a hydrogen bond (O26···I2 = 3.441(5) Å) to one of the coordinated iodine ions and, through this series of cooperative hydrogen bonds, adjacent 1D strands are linked into a 2D brick wall network parallel to (100) (Fig. 8, see Table 2 for details of hydrogen bonding parameters). Each layer is then connected to one other layer by means of offset face-to-face π–π interactions between neighbouring imidazole rings (centroid–centroid distance = 3.569 Å) to form a bilayer (Fig. 9). The second methanol molecule is disordered over two positions; both positions are such that the hydroxyl oxygen atom accepts an N–H···O hydrogen bond from an imidazole amino nitrogen atom (N23). One of the disordered orientations can donate an O–H···I hydrogen bond and the other orientation can accommodate an O–H··· π interaction to a phenylene ring.

### Comparison of structures 1–4

In each complex a 1D polymeric strand is formed in which the Cd-ion is tetrahedrally coordinated to two iodide ions and two nitrogen atoms belonging to separate **L** molecules. It is interesting to note that a 1 : 1 ligand-to-metal ratio persists in all of the solid-state structures, even though the solution ligand-to-metal ratio was varied. Each crystal structure also contains solvent molecules that participate in hydrogen bonding interactions; when the structure contains $H_2O$ or MeOH (*i.e.* **1**, **2** and **4**), 1D strands are formed that link to adjacent strands by virtue of strong solvent-bridged hydrogen bonds; weak π–π interactions served this purpose

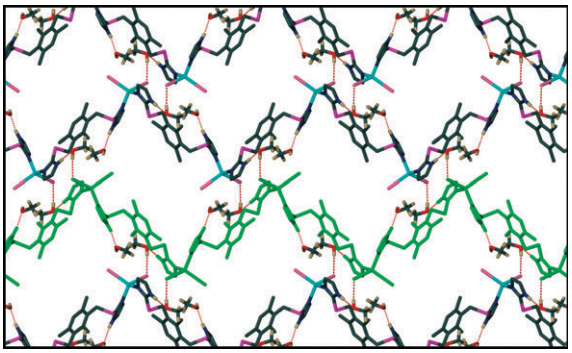

**Fig. 8** Projection perpendicular to (100) of the 2D brick wall network of **4** formed by hydrogen bonding; one 1D strand has been highlighted in green and all molecules are shown in the capped stick representation.

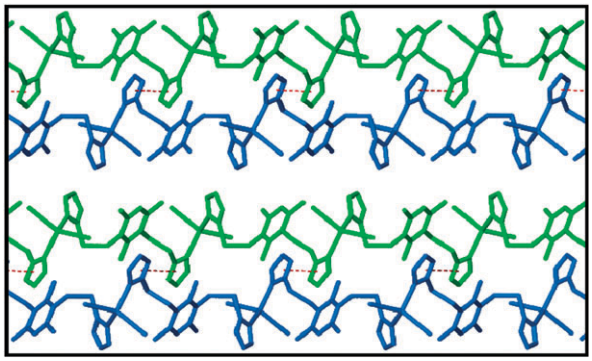

**Fig. 9** The bilayers in **4** as viewed along [010]. π–π interactions are shown as dashed red lines imidazole ring centroids. Separate strands within each bilayers are coloured green and blue. Hydrogen atoms and solvent molecules are omitted for clarity and molecules are shown in the capped-stick metaphor.

in the case of **3** since the $CH_3CN$ solvent can only act as a hydrogen bond acceptor.

The ligand adopts the **UU** conformation in complexes **1**, **2** and **3**. In all three of these structures the amino nitrogen atoms of the imidazole rings donate hydrogen bonds to the solvent molecules, and in this role of bifurcated hydrogen bond acceptor, the solvent molecule most likely stabilises the **UU** conformation. This conformation also facilitates the formation of π–π stacking interactions between phenyl rings of adjacent 1D strands in **2** and **3**, and adjacent 2D layers in **1**. In contrast to **1–3** the two solvent molecules in **4** are not involved in bifurcated hydrogen bonding, instead each MeOH molecule is hydrogen bonded to one uncoordinated nitrogen atom of an imidazole group. The ligand adopts the **UD** conformation, and the benzene rings are not able to participate in π–π stacking interactions.

There are significant similarities in the intermolecular interactions within the crystal structures of all four complexes. A convenient way to view and quantify these intermolecular interactions is by mapping a Hirshfeld surface[11] onto a fragment of each complex using the program CrystalExplorer[12] and then generating the corresponding 2D fingerprint plot.[13] By definition a Hirshfeld surface is a means of dividing space in a crystal into regions of electron density and the actual surface is defined by the portion of space where the promolecule electron density contributes exactly half of the total procrystal electron density (the terms promolecule and procrystal refer to the spherical atoms of the molecule of interest and to the atoms of the whole crystal, respectively).[9] The molecular Hirshfeld surface thus encloses a single molecule within the crystal and provides a smooth surface onto which certain scalar properties (for example, contact distances) can be mapped. For each point on the surface, two distances are defined: $d_i$, the distance from the surface to the nearest atom interior to the surface, and $d_e$, the distance from the surface to the nearest atom exterior to the surface. The 2D fingerprint plot is constructed by binning the $d_i$ and $d_e$ pairs in intervals of 0.01 Å, thereby creating a 2D histogram that reflects all the intermolecular interactions of the molecule. Each bin is coloured according to the fraction of surface points in that bin.[10]

 

In order to generate the surfaces for **1–4**, a single fragment of each complex first needed to be defined; for the purposes of this study a fragment was taken to be a single $CdLI_2$ unit within the 1D coordination polymer chain in each crystal structure. It should be noted that, to date, all examples in the literature that have made use of Hirshfeld surface analyses have done so on crystal structures containing discrete molecules or complexes and that, to the best of our knowledge, ours is the first report of a surface being generated for a fragment comprising a metal–organic unit within a 1D coordination polymer. We also note that this approach must be taken and interpreted with great care since the software is insensitive to the differences between inter- and intramolecular contacts. When two or more polymeric structures are compared and contrasted by means of the Hirshfeld surface analysis, the extended systems should be truncated in a similar manner, and the intramolecular contacts should be clearly indicated.

Based purely on a visual inspection of the fingerprint plots in Fig. 10 it appears that the structures have several features in common but these features are more similar to one another in complexes **1–3** than those in complex **4**. One of the most obvious common features is the sharp spike labelled A in the vicinity of $(d_i, d_e) \approx (0.7, 1.1$ Å). This interaction is attributed to the hydrogen bond between the imidazole amino nitrogen atoms and the solvent molecules *i.e.* the N–H···O hydrogen bond in complexes **1**, **2** and **4** and the N–H···N hydrogen bond in **3** and, as might be expected, a slightly longer interaction is apparent for **3**. A second prominent "interaction" (labelled B) indicates the coordination bond between the Cd and N atoms, which appear as a pair of spikes at the bottom left of the plots (*i.e.* at low $d_i$ and $d_e$ values). The short head-to-head H···H contacts (labelled C) at the limit of the van der Waals radii appear as a characteristic narrow hump between peaks B for complexes **1–4**. The 'wings' at D indicate the H···I hydrogen bonds—the upper wing is associated with the hydrogen bond donor and the lower wing with the hydrogen bond acceptor. In all four of the plots this interaction is coloured blue-green, indicating that a larger proportion of points on the Hirshfeld surface are involved in interactions of this nature.

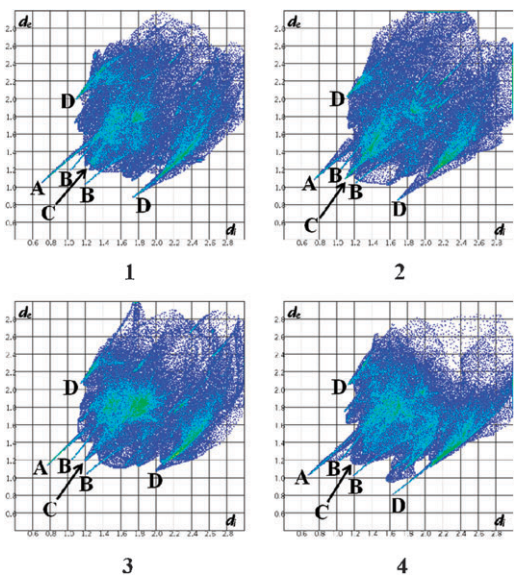


**Fig. 10** Fingerprint plots of complexes **1–4**; refer to text for clarification of the labels.

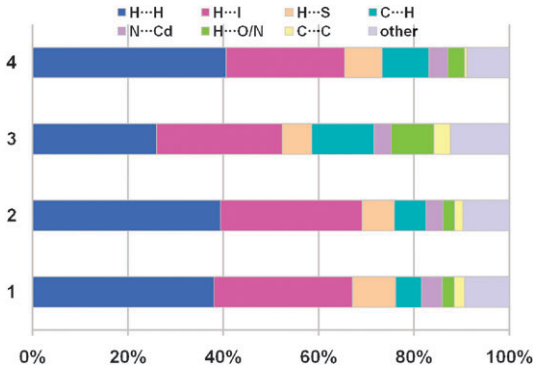


**Fig. 11** Percentage contributions to the Hirshfeld surface area for various contacts in complexes **1–4**.

Fig. 11 contains the percentage contributions for a variety of contacts in the complexes. From these values it can be seen that the C···C contacts, associated with π–π stacking interactions in the $(d_i, d_e) \approx (1.8, 1.8$ Å) region, are minimal in **4** (only 0.5% of the surface is due to C···C interactions compared with the 2.2, 1.8 and 3.5% for **1**, **2** and **3**, respectively); this quantitatively verifies observations that are obvious from inspecting the different structures. However, it is interesting to note that the H···S contacts are associated with a significant percentage of the surface area (9.0, 6.8, 6.2 and 7.9% for **1**, **2**, **3** and **4**, respectively), a feature that might otherwise have gone unnoticed if the packing had been analysed by inspection alone.

## Conclusion

In summary, a novel conformationally flexible ditopic ligand was synthesised and reacted with $CdI_2$ under varying conditions to yield four new solvates consisting of 1D coordination polymeric strands. These four complexes were characterised structurally by single crystal X-ray diffraction, which reveals that complex **1** contains a single water molecule that participates in hydrogen bonding to link the 1D polymeric strands into a distorted 2D honeycomb network, whereas complex **2** contains a single MeOH molecule that participates in hydrogen bonding that connects adjacent strands into bilayers. Complex **3** contains two MeCN molecules; however it is the weaker π–π interactions that serve to connect neighbouring strands. Although complex **4** contains two molecules of MeOH, only one is utilised to connect the 1D strands into a 2D brick-wall network. These structures imply that it is not only the nature of solvent molecule that affects the packing arrangement, but that subtle changes in the conformation of the ligand results in variation in the crystal packing.

Finally, we have shown that the fingerprint plots generated by CrystalExplorer provide a convenient means of visualising and comparing the intermolecular interactions of a series of structurally related polymeric complexes.

## Experimental

All reagents and solvents were purchased and used as received. IR spectra were recorded on a Nexus 670 FT-IR instrument (Thermo Nicolet Instruments, USA) in the spectral range 4000–400 $cm^{-1}$ using the KBr pellet method. LC ESI-MS analysis was carried out on a Waters API Quattro Micro mass spectrometer with an electrospray ionisation source and $^{1}$H-NMR and $^{13}$C-NMR spectra were recorded on a Varian Unity INOVA (400 MHz).

### Synthesis of 1,3-bis(1-imidazolyl-2-thione)-2,4,6-trimethylbenzene (L)

2-Mercaptoimidazole (2.01 g, 20 mmol) was added to 2,4-bis(chloromethyl)-1,3,5-trimethylbenzene (1.09 g, 5.0 mmol) in 200 mL of MeOH. The resulting solution was refluxed for 24 h. The solvent was then removed under reduced pressure and yielded a yellow oil, to which $K_2CO_3$ (6.91 g, 50 mmol) in 100 mL of $H_2O$ was added. The solution was stirred until the product precipitated. The white solid was then filtered, washed with 100 mL $H_2O$ and left to air dry. Yield: 92.5%. Mp: 168–170 °C; IR (KBr pellet): $\nu_{max}$ 3434 (N-H of Im), 2363, 1858, 1605 (aromatic C=C), 1547, 1414 ($CH_2$ bend), 1232 ($CH_2$–S wag), 1096, 963, 746 $cm^{-1}$; $^{1}$H-NMR (DMSO-$D_6$, 400 MHz): $\delta$ 2.18 (3H, s, $ArCH_3$), 4.14 (4H, s, $CH_2S$), 6.91 (2H, s, $ArH_a$), 6.94 (1H, s, $ArH_b$), 7.05 (4H, s, CN(H)CHCHN); $^{13}$C-NMR (DMSO-$D_6$, 75.5 MHz): $\delta$ 20.69, 37.6, 123.7, 126.1, 137.5, 137.7, 138.3; MS (ESI+): $m/z$ 317 (100%, $[(M + H]^+)$], 218 (20%, $M^+ -$ SIm), 159 (87%).

### Preparation of complexes 1–4

**Synthesis of $\{[CdLI_2]\cdot H_2O\}_n$ (1).** 10.1 mg **L** (0.029 mmol) was dissolved in 3 mL of MeOH and added to 10.6 mg (0.029 mmol) $CdI_2$ dissolved in 2 mL MeOH. The solvent was allowed to evaporate slowly and after a period of 3 weeks colourless crystals formed, and the structure was elucidated by single-crystal X-ray diffraction.

**Synthesis of $\{[CdLI_2]\cdot CH_3OH\}_n$ (2).** 20.2 mg **L** (0.058 mmol) was dissolved in 3 mL of MeOH and added to 10.6 mg (0.029 mmol) $CdI_2$ dissolved in 2 mL MeOH. The solvent was allowed to evaporate slowly and after a period of one month colourless crystals formed, and the structure was elucidated by single-crystal X-ray diffraction.

**Synthesis of $\{[CdLI_2]\cdot 2CH_3CN\}_n$ (3).** 10.1 mg **L** (0.029 mmol) was dissolved in 3 mL of MeCN and added to 10.6 mg (0.029 mmol) $CdI_2$ dissolved in 2 mL MeCN. The solvent was allowed to evaporate slowly and after a period of 2 weeks colourless crystals formed, and the structure was elucidated by single-crystal X-ray diffraction.

**Synthesis of $\{[CdLI_2]\cdot 2CH_3OH\}_n$ (4).** 10.1 mg **L** (0.029 mmol) was dissolved in 3 mL of MeOH and added to 21.2 mg (0.058 mmol) $CdI_2$ dissolved in 2 mL MeOH. The solvent was allowed to evaporate slowly and after a period of 3 weeks colourless crystals formed, and the structure was elucidated by single-crystal X-ray diffraction.

### X-Ray crystallography

Single crystals of compounds **1–4** were harvested directly from the slow evaporation preparations and in all cases suitable single crystals (*i.e.* those found by inspection to have well-defined morphology and that extinguished plane polarised light uniformly) were attached to the end of a MiTeGen mount using paratone oil. Intensity data were collected on a Bruker SMART Apex CCD single-crystal X-ray diffractometer[14] equipped with an Oxford Cryosystems Cryostream Plus cooling system set at 100 K. The system was operated at 1.2 kW power (40 kV, 30 mA) using monochromated Mo-K$\alpha$ radiation ($\lambda$ = 0.71073 Å). Data reduction was carried out by means of a standard procedure using the Bruker SAINT software package.[15] Where necessary, empirical corrections were performed using SADABS.[16,17] All crystal structures were solved and refined using SHELX-97.[18] X-Seed[19] was used as a graphical interface for SHELX. Structures were solved either by direct methods or a combination of Patterson methods and partial structure expansion using SHELXS-97. Structures were expanded by iterative examination of difference Fourier maps following least squares refinements of earlier models. All non-hydrogen atoms were refined anisotropically by means of full-matrix least squares calculations on $F^2$ using SHELXL-97. Where appropriate, hydrogen atoms were placed in calculated positions using riding models and assigned isotropic thermal parameters 1.2–1.5 times $U_{eq}$ of their parent atoms. Hydroxyl and water hydrogen atoms were located in difference electron density maps and refined independently.

**Crystal data for 1.** $C_{17}H_{22}CdI_2N_4OS_2$, $M$ = 728.71, colourless plate, 0.11 × 0.09 × 0.06 mm, monoclinic, space group $P2_1/c$ (No. 14), $a$ = 13.470(3), $b$ = 11.610(3), $c$ = 15.371(3) Å, $\beta$ = 99.904(4)°, $V$ = 2367.9(9) Å$^3$, $Z$ = 4, $D_c$ = 2.044 g cm$^{-3}$, $F_{000}$ = 1384, Mo-K$\alpha$ radiation, $\lambda$ = 0.71073 Å, $T$ = 100(2) K, $2\theta_{max}$ = 56.5°, 14 624 reflections collected, 5506 unique ($R_{int}$ = 0.0349). Final *GooF* = 1.076, $R1$ = 0.0378, w$R2$ = 0.0827, $R$ indices based on 4801 reflections with $I > 2\sigma(I)$ (refinement on $F^2$), 255 parameters, 3 restraints. Lp and absorption corrections applied, $\mu$ = 3.720 mm$^{-1}$.

**Crystal data for 2.** $C_{18}H_{24}CdI_2N_4OS_2$, $M$ = 742.73, 0.24 × 0.17 × 0.11 mm, monoclinic, space group $C2/c$ (No. 15), $a$ = 31.625(3), $b$ = 11.0517(10), $c$ = 16.3433(15) Å, $\beta$ = 119.0840(10)°, $V$ = 4992.0(8) Å$^3$, $Z$ = 8, $D_c$ = 1.977 g cm$^{-3}$, $F_{000}$ = 2832, Mo-K$\alpha$ radiation, $\lambda$ = 0.71073 Å, $T$ = 100(2) K, $2\theta_{max}$ = 56.6°, 15 354 reflections collected, 5813 unique ($R_{int}$ = 0.0339). Final *GooF* = 1.060, $R1$ = 0.0396, w$R2$ = 0.0885, $R$ indices based on 4948 reflections with $I > 2\sigma(I)$ (refinement on $F^2$), 258 parameters, 0 restraints. Lp and absorption corrections applied, $\mu$ = 3.532 mm$^{-1}$.

**Crystal data for 3.** $C_{21}H_{22}CdI_2N_6S_2$, $M$ = 792.80, 0.180 × 0.120 × 0.080 mm, triclinic, space group $P\bar{1}$ (No. 2), $a$ = 9.6481(9), $b$ = 11.2186(10), $c$ = 14.1622(13) Å, $\alpha$ = 112.0230(10), $\beta$ = 91.681(2), $\gamma$ = 101.926(2)°, $V$ = 1380.7(2) Å$^3$, $Z$ = 2, $D_c$ = 1.907 g cm$^{-3}$, $F_{000}$ = 760, Mo-K$\alpha$ radiation, $\lambda$ = 0.71073 Å, $T$ = 100(2) K, $2\theta_{max}$ = 56.6°, 16 003 reflections collected, 6381 unique ($R_{int}$ = 0.0425). Final *GooF* = 1.080,

 

$R1$ = 0.0478, w$R2$ = 0.1147, $R$ indices based on 5475 reflections with $I > 2\sigma(I)$ (refinement on $F^2$), 294 parameters, 0 restraints. Lp and absorption corrections applied, $\mu$ = 3.198 $mm^{-1}$.

**Crystal data for 4.** $C_{19}H_{28}CdI_2N_4O_2S_2$, $M$ = 774.77, 0.22 × 0.10 × 0.07 mm, monoclinic, space group $C2/c$ (No. 15), $a$ = 32.585(4), $b$ = 10.2983(14), $c$ = 19.944(3) Å, $\beta$ = 125.829(2)°, $V$ = 5426.1(13) $Å^3$, $Z$ = 8, $D_c$ = 1.897 g $cm^{-3}$, $F_{000}$ = 2976, Mo-K$\alpha$ radiation, $\lambda$ = 0.71073 Å, $T$ = 100(2) K, $2\theta_{max}$ = 56.7°, 16 699 reflections collected, 6331 unique ($R_{int}$ = 0.0525). Final *GooF* = 1.068, $R1$ = 0.0567, w$R2$ = 0.1080, $R$ indices based on 4832 reflections with $I > 2\sigma(I)$ (refinement on $F^2$), 278 parameters, 7 restraints. Lp and absorption corrections applied, $\mu$ = 3.256 $mm^{-1}$.

## Acknowledgements

We thank the National Research Foundation and the Department of Science and Technology for support of this work.

## Notes and references

1 (*a*) P. J. Langley and J. Hulliger, *Chem. Soc. Rev*., 1999, **28**, 279; (*b*) G. R. Desiraju, *Crystal Engineering, the Design of Organic Solids*, Elsevier, Amsterdam, 1989; (*c*) A. S. Batsanov, J. C. Collings, R. M. Ward, A. E. Goeta, L. Porres, A. Beeby, J. K. Howard, J. W. Steed and T. B. Marder, *CrystEngComm*, 2006, **8**, 622.
2 (*a*) L. Dobrzańska, G. O. Lloyd, H. G. Raubenheimer and L. J. Barbour, *J. Am. Chem. Soc*., 2006, **128**, 698; (*b*) P. Sozzani, S. Bracco, A. Comotti, L. Feretti and R. Simonutti, *Angew. Chem., Int. Ed*., 2005, **44**, 1816; (*c*) S. Norro, S. Kitagawa, M. Kondo and K. Seki, *Angew. Chem., Int. Ed*., 2000, **39**, 2081; (*d*) H. Li, M. Eddaoudi, M. O'Keeffee and O. M. Yaghi, *Nature*, 1999, **402**, 276.
3 (*a*) L. R. MacGillivray, J. L. Reid and J. A. Ripmeester, *J. Am. Chem. Soc*., 2000, **122**, 7817; (*b*) K. Tanaka and F. Toda, *Chem. Rev*., 2000, **100**, 1025.
4 (*a*) B. Moulton and M. J. Zaworotko, *Chem. Rev*., 2001, **101**, 1629; (*b*) C. Janiak, *Dalton Trans*., 2003, 2781; (*c*) G. R. Desiraju, *J. Mol. Struct*., 1996, **374**, 191.
5 G. C. Xu, Y. J. Ding, T. A. Okamura, Y. Q. Huang, G. X. Liu, W. Y. Sun and N. Ueyama, *CrystEngComm*, 2008, **10**, 1052.
6 B. Sui, J. Fan, T. A. Okamura, W. Y. Sun and N. Ueyama, *Solid State Sci*., 2005, **7**, 969.
7 (*a*) L. Dobrzańska, D. J. Kleinhans and L. J. Barbour, *New J. Chem*., 2008, **32**, 813; (*b*) L. Dobrzańska, G. O. Lloyd and L. J. Barbour, *New J. Chem*., 2007, **31**, 669; (*c*) L. Dobrzańska, G. O. Lloyd, T. Jacobs, I. Rootman, C. L. Oliver, M. W. Bredenkamp and L. J. Barbour, *J. Mol. Struct*., 2006, **796**, 107; (*d*) L. Dobrzańska, H. G. Raubenheimer and L. J. Barbour, *Chem. Commun*., 2005, 5050; (*e*) G. O. Lloyd, J. Alen, M. W. Bredenkamp, E. J. de Vries, C. Esterhuysen and L. J. Barbour, *Angew. Chem., Int. Ed*., 2006, **45**, 5354; (*f*) L. Dobrzańska, G. O. Lloyd, H. G. Raubenheimer and L. J. Barbour, *J. Am. Chem. Soc*., 2005, **127**, 13134; (*g*) L. Dobrzańska, G. O. Lloyd, H. G. Raubenheimer and L. J. Barbour, *J. Am. Chem. Soc*., 2006, **128**, 698.
8 (*a*) R. Banerjee, A. Phan, B. Wang, C. Knobler, H. Furukawa, M. O'Keeffee and O. M. Yaghi, *Science*, 2008, **319**, 939; (*b*) C. Y. Su, Y. P. Cai, C. L. Chen, M. D. Smith, W. Kaim and H. C. zur Loye, *J. Am. Chem. Soc*., 2003, **125**, 8595; (*c*) C. Y. Su, Y. P. Cai, C. L. Chen, F. Lissner, B. S. Kang and W. Kaim, *Angew. Chem., Int. Ed*., 2002, **41**, 3371.
9 F. L. Hirshfeld, *Theor. Chim. Acta*, 1977, **44**, 129.
10 M. A. Spackman and D. Jayatilaka, *CrystEngComm*, 2009, **11**, 19.
11 M. A. Spackman and P. G. Byrom, *Chem. Phys. Lett*., 1997, **267**, 215.
12 S. K. Wolff, D. J. Grimwood, J. J. McKinnon, D. Jayatilaka and M. A. Spackman, *CrystalExplorer 2.1*, University of Western Australia, Perth, 2007.
13 M. A. Spackman and J. J. McKinnon, *CrystEngComm*, 2002, **4**, 378.
14 SMART Data Collection Software, Version 5.629, Bruker AXS Inc., Madison, WI, 2003.
15 SAINT Data Collection Software, Version 6.45, Bruker AXS Inc., Madison, WI, 2003.
16 SADABS, Version 2.05, Bruker AXS Inc., Madison, WI, 2002.
17 R. H. Blessing, *Acta Crystallogr., Sect. A: Found. Crystallogr*., 1995, **51**, 33.
18 G. M. Sheldrick, *Acta Crystallogr., Sect. A: Found. Crystallogr*., 2008, **64**, 112.
19 L. J. Barbour, *J. Supramol. Chem*., 2001, **1**, 189.